PHYSICAL REVIEW E VOLUME 61, NUMBER 3 MARCH 2000

Scale-invariant fluctuations at different levels of organization in developing heart cell networks

Yoav Soen and Erez Braun
Physics Department, Technion–Israel Institute of Technology, 32000 Haifa, Israel
(Received 10 May 1999)

In the last few years it has been realized that the intervals of spontaneous spiking events in the intact heart exhibit coexisting scale-invariant count fluctuations and anticorrelated interspike interval fluctuations. Here, we show experimentally that this feature is an intrinsic property of single isolated heart cells, which is preserved when the cells couple into networks. We present a model explaining this behavior at both the single cell and network levels.

PACS number(s): 87.19.Hh, 05.40.−a, 87.15.Ya

Physiological systems were traditionally thought to obey the homeostasis principle, whereby they organize to reduce fluctuations. However, application of time series analysis techniques to long spike trains recorded from the intact heart [1] and various neural systems [2] reveal asymptotic power-law increase of fluctuations as a function of the size of the statistical window. The intact heart fluctuations are associated with long-range anticorrelations [3] and are commonly attributed to its neuronal control [3,4]. Here, by applying a noninvasive recording technique [5] to spontaneously beating heart cells *in vitro*, we show that coexisting scale-invariant (count) fluctuations (SIF) and long-range anticorrelations of interspike interval (ISI) displacements are intrinsic to single isolated heart cells. Furthermore, the anticorrelations are more dominant at the network level, accounting for its ability to eliminate stochastic occurrences of long time intervals with no beating (i.e., quiescent periods) that are commonly observed in isolated cells. This difference between isolated cells and dense networks suggests that an isolated cell pacemaker is unlikely. Based on these findings and previous experimental [6] and theoretical [7,8] studies we propose a model incorporating history-dependent inactivation into the excitable machinery of single cells. This model couples the ion-channel kinetics, underlying the single cell activity, to the excitable network in a natural way, exhibiting similar SIF in both single cells and networks. It also includes an intrinsic feedback mechanism introducing long-range anticorrelations responsible for maintaining a stable rhythm, despite the SIF.

Experiments were performed on cultures of spontaneously beating ventricular cells from newborn rats [5,9]. Isolated cells are plated at the desired density on collagen coated glass petri-dish and cultured on the stage of an inverted microscope under sterile incubating conditions of $37\pm0.2\,^{\circ}\mathrm{C}$ and 6% CO_2. Cell population comprises contracting cells (myocytes), as well as noncontracting connective tissue cells (fibroblasts). Following plating, the cells proliferate (mostly fibroblast cells), migrate, and connect to form confluent monolayer of cells (in about one week), which later becomes a network of fibers (usually within two weeks). The cells within the network are coupled electrically via Gap-junction connections, that can be viewed, to a first approximation, as ohmic conduction paths. Yet, the fibroblasts are passive and do not actively participate in spike generation. By controlling the initial plating density of myocytes, different levels of organization can be explored, namely: isolated cells, small groups of cells, and networks with various densities and morphologies. The measurement is based on the acquisition of the optical field of view to a computer performing real-time motion detection. It enables continuous recording of spontaneous contractions from all levels of *in vitro* organization over a wide range of time scales (up to several weeks) with high spatiotemporal resolution.

In general, isolated cells are characterized by relatively irregular beating, with stochastic occurrences of long quiescent periods, while dense networks of cells usually exhibit synchronized rhythmic behavior, which is spontaneously disrupted by complex rhythm disorders [5]. Here, we first demonstrate SIF on traces that do not exhibit strong irregularities, and then show it also for those records that include strong beating disorders. To detect and estimate SIF, we use the Allan factor (AF) measure [10]. It is applied to the sequence of counts $N_T(i)$ obtained by counting the number of spikes (i.e., contractions) $N_T(i)$ within contiguous bins of length T. The AF is defined as

$$A(T)\equiv\frac{E\{[N_T(i+1)-N_T(i)]^2\}}{2E[N_T(i)]}.$$

In the presence of scale-invariant fluctuations, the AF asymptotically increases as T^{α}. The exponent α is bounded to the range $0\leqslant\alpha\leqslant3$ and provides a measure for the relative strength of fluctuations over various time scales. The increase in AF reflects an ordering of spiking events in ever growing clusters, implying that, at least within the power-law range, the ISIs are correlated over all the time scales so that each ISI depends on the entire past activity. Figure 1 summarizes four exemplary AF plots of relatively regular records (insets) from four different organization levels, namely: a single isolated cell (a), four coupled cells embedded within a passive tissue (b), monolayered network (c), and a network of fibers (d).

These records exhibit a reduction of fluctuations on short time scales (1–100 sec) and a power-law increase in the asymptotic region, with a scaling exponent $\alpha\approx2$ (note that for the intact heart $0<\alpha<2$ [11]). Other records (of at least 15 000 events each) from different cultures at different densities reveal α in the range 1.5 to 2.1. The variance in α (which seems to be wider for single cells) stems from the inherent randomness of the fluctuations strength so that dif-

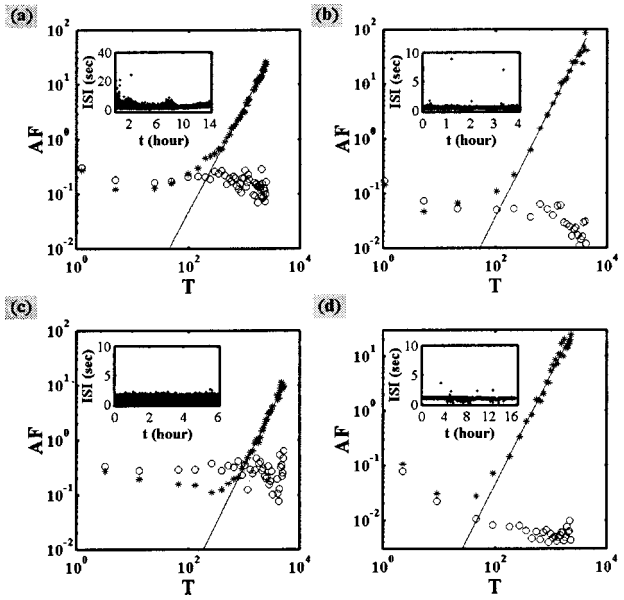

FIG. 1. Allan factor of the raw (stars) and shuffled (circles) data computed for regular traces from four different organization levels: (a) single isolated cell ($\alpha=1.92$), (b) four coupled cells embedded within a passive tissue ($\alpha=2.02$), (c) regularly beating monolayered network ($\alpha=2.07$), and (d) a network of fibers ($\alpha=2.01$). The time window T is normalized by the $mean(ISI)$. The insets show the ISI traces, for which the AFs were computed.

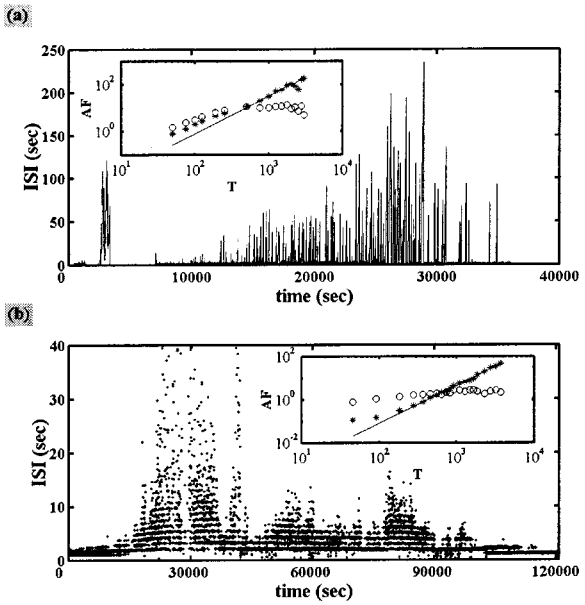

FIG. 2. Two ISI traces exhibiting typical single cell (a) and network (b) disorders. The data points in (a) are joined with lines to emphasize the quiescent periods (vertical lines) of up to 230 sec. The bands structure in (b) reflects a modulated skipped beats pattern (shown also in [5]). The corresponding AFs in the insets exhibit asymptotic scaling with exponents [$\alpha=1.6$ in (a) and $\alpha=1.75$ in (b)] that fall within the same range of α as that obtained for the regular traces. The time window T is normalized by the fundamental period.

ferent instances of the same process may yield slightly different exponents [10]. As expected, random shuffling of the ISIs destroys all the ordering correlations and eliminates the scaling (circles). Examination of irregular records from single cells, exhibiting stochastic quiescent periods [Fig. 2(a)], as well as from networks, exhibiting complex rhythm disorders [Fig. 2(b)], reveals asymptotic SIF regardless of the particular dynamics on short time scales.

Since the exponent α relates to the fluctuations of counts and does not convey all the information about the nature of ISI fluctuations, we follow the method introduced in [3] and compute, for each ISI trace, the mean ''difference'' $\Delta S(n)$ between two ISIs separated by n events,

$$\Delta S(n) \equiv \overline{abs[S(n+m)-S(m)]},$$

where $S(n)$ is the nth ISI and the bar denotes an average over all m values. For uncorrelated ISI fluctuations (as for Brownian noise), $\Delta S(n) \sim n^{1/2}$. A weaker dependence on n indicates that the fluctuations in ISI are anticorrelated. Figure 3(a) shows representative log-log plots of $\Delta S(n)$ for a single isolated cell and a monolayered network.

Indeed, the single isolated cell (pluses) exhibits a flat slope (below 1/2) for separations less than about 3000 events, indicating the presence of strong anticorrelation, acting to reduce ISI differences. Beyond 3000 events, the slope is higher but still below 1/2. The network exhibits a flat slope for all separations (stars), in agreement with the elimination of the quiescent periods.

Scale-invariant statistics have also been demonstrated for voltage-gated ion-channels [12,13] and were associated with the degeneracy of their states [7]. Recent experiments (including on sodium channels from heart muscle cells) re-

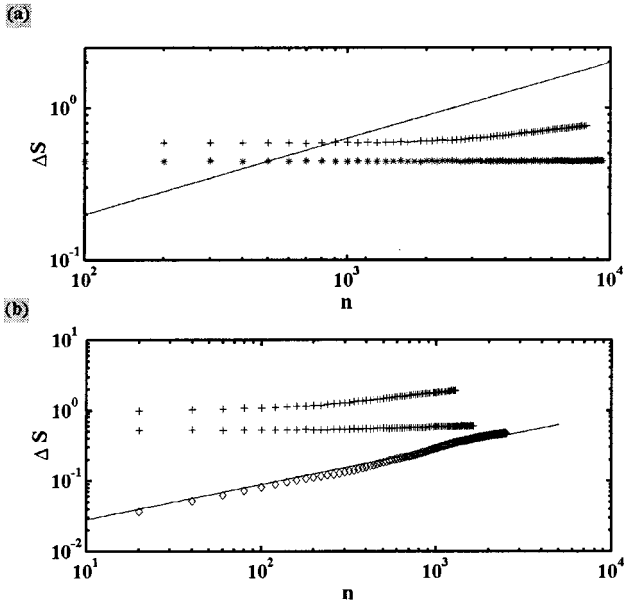

FIG. 3. Average difference $\Delta S(n)$ between ISI pairs separated by n events (in a log-log scale). (a) Experimental results for a typical network (stars) and a single isolated cell (pluses). (b) Simulation results for the isolated cell model with $\delta/\lambda=4$ (pluses, lower curve), $\delta/\lambda=1$ (pluses, higher curve) and for a simple Brownian motion (diamonds). For all cases $\alpha \approx 2$, yet ΔS depends differently on n, yielding asymptotic slopes of 0.07, 0.32, and 0.56, respectively. Dashed lines represent a slope of 1/2.

vealed a power-law statistics associated with the recovery of channels from inactivation [6,12]. Here we introduce a mechanism of activity dependent inactivation at the single cell level. The model incorporates an inactivation variable with history-dependent kinetics, into the excitable machinery of the cell. It is based on a modification of the Morris Lecar (ML) nonlinear oscillator [14], with two oscillatory variables v and w, to which we add a much slower dynamical variable $0<p<1$, denoting the relative degree of cell inactivation. This variable could be thought of as representing the overall effect on the cell induced by an unavailable pool of inactivated ion-channels (i.e., voltage-gated channels that temporarily become nonconducting and voltage-insensitive). Except for the introduction of a dynamic exciting conductance $g_E(t)$, v and w evolve according to the standard ML equations,

$$\frac{dv}{dt} = -g_E(t)m_\infty(v)(v-1) - \bar{g}_R w(v-v_R) - \bar{g}_L(v-v_L) + I_{ext} + I_{coup},$$

$$\frac{dw}{dt} = \phi\frac{[w_\infty(v)-w]}{\tau_w(v)},$$

$$g_E(t) = \bar{g}_E(1-p).$$

Here ϕ is a rate parameter, $\bar{g}_E$, $\bar{g}_R$, $\bar{g}_L$, v_R, and v_L are maximal conductances and normalized reversal potentials of an exciting, restoring, and leak currents respectively, and m_∞, w_∞, and τ_w are functions of v [15]. Positive I_{ext} is required for an oscillatory solution of the (v,w) subsystem and I_{coup} represents the coupling to other cells. The dynamic conductance $0<g_E(t)<\bar{g}_E$ depends on the degree p of cell inactivation. Motivated by recent reports [12,6], we let the kinetics of p reflect an hierarchy of inactivation states. Random, voltage-independent transitions among these states are allowed. However, since some states are considered more inactive than others, only a fraction p_{eff} of the channels can recover, at a given time, to the available, voltage-sensitive pool and contribute to the exciting conductance. In order to simulate this fraction, we introduce an arbitrary state reporter $0<r(t)<\infty$, comprising the absolute value of a sum of random displacements. It denotes the inactivation ''depth'' (i.e., some distance measure in inactivation space) and is implemented by integrating a white noise term $\xi(\tau)$, i.e., $r(t) = abs[\int_0^t \xi(\tau)d\tau]$. The higher the state of the reporter $r(t)$, the deeper is the inactivation of the cell (and the smaller the effective recovery rate). The simplest construction of p_{eff}, so that $0<p_{eff}<p$, is $p_{eff}=p/1+r(t)$. The kinetic equation for p is then

$$\frac{dp}{dt} = \lambda w(1-p) - \delta\frac{p}{1+r(t)}.$$

It consists of a deterministic term $\lambda w(1-p)$ [or alternatively, $\lambda m_\infty(v)(1-p)$, a choice that leave the results of the model intact], representing the rate of inactivation and a recovery term $\delta[p/1+r(t)]$, that is dependent on the effective population p_{eff}. Note that the model relies on basic ion-channel phenomenology and is not intended to describe the microscopic details of a specific cell.

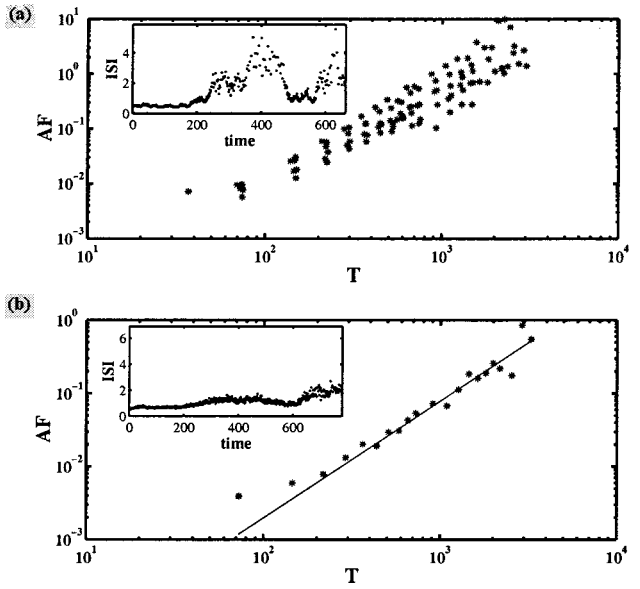

FIG. 4. Model AF plots of (a) six isolated cells, with different white-noise seeds and (b) their strongly coupled network version. The time window T is normalized by the $mean(ISI)$. The variance of α in (a) is due to different seeds and its average is close to the network exponent in (b) ($\alpha=1.6$ and $\alpha=1.59$, respectively). A different choice of model parameters can lead to less regular ISI traces (insets), almost without affecting the scaling exponent. The ISI and time axes are normalized by the $mean(ISI)$.

The coupling among cells I_{coup} is introduced by a sum (over all the cells in contact) of independent ohmic currents $I_{coup}=\Sigma K_j(v_j-v)$, where K_j is the coupling strength to cell j. Figure 4 shows AF plots computed from simulated spike trains of six isolated cells [Fig. 4(a)] and a ringlike network formed by a symmetrical coupling between each of these cells and its two nearest-neighbors [Fig. 4(b)]. Apart from different seeds used for generating the random numbers ξ, all the model cells are identical [16]. The coupling of cells within the network is strong enough to enforce complete synchronization of them.

The AFs exhibit a scaling behavior with seed-dependent exponents [$mean(\alpha)=1.6$ for the single cell and $\alpha=1.59$ for the network] that fall within the experimental regime. Repeating the simulations with some other, randomly chosen parameters [e.g., $\bar{g}_E$, λ, δ, and $std(\xi)$], or other oscillator models than ML, indicates that α is weakly dependent on the specific choice of the oscillator. As expected, the removal of the Brownian reporter eliminates the scale-invariant behavior. Yet, in contrast to the standard Brownian motion, the coupling to the nonlinear excitable machinery of the cells introduces anticorrelations to the ISI fluctuations. The reason for this is that the loss of channels depends on spiking activity, whereas the recovery is independent of it. Consequently, high reporter values lead to long ISIs followed by a decrease in channel inactivation (without affecting the recovery), which, in turn, increases the excitability (i.e., shortens the ISIs). Hence, the model conveys an effective restoring force, acting to decrease the flow of channels into the inactive states (not to be confused with a biased Brownian motion, wherein the force acts on the walker itself). The strength of

this negative feedback depends on δ/λ (besides, of course, the reporter state). Increasing this ratio results in a stronger anticorrelation, without affecting the exponent α. Figure 3(b) shows exemplary plots of $\Delta S(n)$ for a single cell model with two different δ/λ ratios (pluses) and for a trace of a simple Brownian motion (diamonds). Indeed, the asymptotic slopes of $log[\Delta S(n)]$ for both model traces are below 1/2 and are inversely related to δ/λ, indicating stronger anticorrelation for larger δ/λ. Furthermore, the negative feedback is expected to be more effective at the network level, due to the ability of cells to share resources; whenever a particular cell loses its excitability [e.g., for high $r(t)$ values], it responds in a quiescent period that can be eliminated by the strong coupling to other, more excitable (on the average) cells. Indeed, a comparison of the ISI traces generated by the single cell and small network (up to six cells) models shows that a single cell is more prone to exhibit quiescent periods (Fig. 4, insets).

In summary, nontrivial scale-invariant fluctuations underlie the activity at all levels of heart-cell organization (from ion-channels to the intact organ) and may account for broadband modulations of spontaneous beating disorders. The SIF coexist with long-range anticorrelations that, in single isolated cells, are insufficient to maintain continuous beating. However, when the cells are strongly coupled in a dense network, the anticorrelations are amplified, thus preventing the ISIs from becoming too large. The model presented provides a simple, neural-free explanation for the presence of scale-invariant anticorrelations. It explains why the cooperation of many beating cells (e.g., in the heart pacemaker region) is required for maintaining a tolerable ISI variance.

We thank S. Marom for valuable discussions and N. Cohen for participating in the experiments. This work has been supported by the U.S.-Israel Binational Science Foundation, Grant No. 94-262.

[1] P. C. Ivanov, M. G. Rosenblum, C. K. Peng, J. Mietus, S. Havlin, H. E. Stanley, and A. L. Goldberger, Nature (London) **383**, 323 (1996); C. K. Peng, S. Havlin, H. E. Stanley, and A. L. Goldberger, Chaos **5**(1), 82 (1995); R. G. Turcott and M. C. Teich, Ann. Biomed. Eng. **24**, 269 (1996).

[2] S. B. Lowen and M. C. Teich, J. Acoust. Soc. Am. **99**, 3585 (1996); M. C. Teich, C. Heneghan, S. B. Lowen, T. Ozaki, and E. Kaplan, J. Opt. Soc. Am. A **14**, 529 (1997); R. G. Turcott, P. D. R. Barker, and M. C. Teich, J. Stat. Comput. Simul. **52**, 253 (1995).

[3] C. K. Peng, J. Mietus, J. M. Hausdorff, S. Havlin, H. E. Stanley, and A. L. Goldberger, Phys. Rev. Lett. **70**, 1343 (1993).

[4] B. J. West and W. Deering, Phys. Rep. **246**, 1 (1994).

[5] Y. Soen, N. Cohen, D. Lipson, and E. Braun, Phys. Rev. Lett. **82**, 3556 (1999).

[6] A. Toib, V. Lyakhov, and S. Marom, J. Neurosci. **18**, 1893 (1998); M. M. Frank and S. Marom, Eur. J. Phys. **438**, 213 (1999).

[7] G. L. Millhauser, E. E. Salpeter, and R. E. Oswald, Proc. Natl. Acad. Sci. USA **85**, 1503 (1988).

[8] S. B. Lowen, L. S. Liebovitch, and J. A. White, Phys. Rev. E **59**, 5970 (1999).

[9] N. Cohen, Y. Soen, and E. Braun, Physica A **249**, 600 (1998).

[10] S. Thurner, S. B. Lowen, M. C. Feurstein, H. G. Feichtinger, and M. C. Teich, Fractals **5**, 565 (1997).

[11] G. M. Viswanathan, C. K. Peng, H. E. Stanley, and A. L. Goldberger, Phys. Rev. E **55**, 845 (1997).

[12] S. Marom, J. Membr. Biol. **161**, 105 (1998), and references therein.

[13] L. S. Liebovitch and J. M. Sullivan, Biophys. J. **52**, 979 (1987); G. L. Millhauser, E. E. Salpeter, and R. E. Oswald, *ibid.* **54**, 1165 (1988).

[14] J. Rinzel and G.B. Ermentrout, in *Methods in Neuronal Modeling*, edited by C. Koch and I. Segev (MIT Press, Cambridge, MA, 1989), p. 167.

[15] $m_\infty(v)=1/2\{1+\tanh[(v+0.01)/0.15]\}$, $w_\infty(v)=1/2\{1+\tanh[(v-0.1)/0.145]\}$, and $\tau_w(v)=\cosh[(v-0.1)/0.29]$.

[16] Model parameters are $I_{\rm ext}=0.1$, $\overline{g_E}=1$, $\overline{g_R}=2$, $\overline{g_L}=0.5$, $v_l=-0.5$, $v_k=-0.7$, $\phi=0.8$, $\lambda=0.01$ [0.04 in the second trace of Fig. 3(b)], $\delta=0.01$, $std(\xi)=0.01$, and $K=5$. The inset traces are obtained by changing $\overline{g_E}$, λ, δ, and $std(\xi)$ to 0.85, 0.02, 0.02, and 0.1, respectively. A (nonintegrated) white noise term ($SD=0.005$) was added to the parameter ϕ in order to generate noisier traces that look more like the experimental ones. This has no effect on the scaling.